JOURNAL OF CHEMICAL EDUCATION

pubs.acs.org/jchemeduc Article

A Primer on Lattice Planes, Crystal Facets, and Nanoparticle Shape Control

Anne K. Bentley and Sara E. Skrabalak*

Cite This: *J. Chem. Educ.* 2023, 100, 3425−3433 Read Online

ACCESS | Metrics & More | Article Recommendations | Supporting Information

ABSTRACT: An exciting recent development in chemistry has been the ability to control nanoparticle crystal morphology or shape. Nanoparticles of different shapes present different crystal surfaces (or facets) with respect to the surrounding environment. Synthetic control over nanoparticle morphology has enabled the study of the influence of surface facets on the catalytic properties of nanoparticles. Here, these recent advances are leveraged as a theme to introduce and review the use of Miller indices to describe crystal planes, facets, and directions of growth of metal nanoparticles. Inexpensive paper and 3D printed models of metal nanoparticle cubes, rhombic dodecahedra, and octahedra bound by the low-index lattice planes of the face-centered cubic crystal structure are included. Nanoparticle shape control provides an accessible introduction to materials chemistry topics for students at all levels.

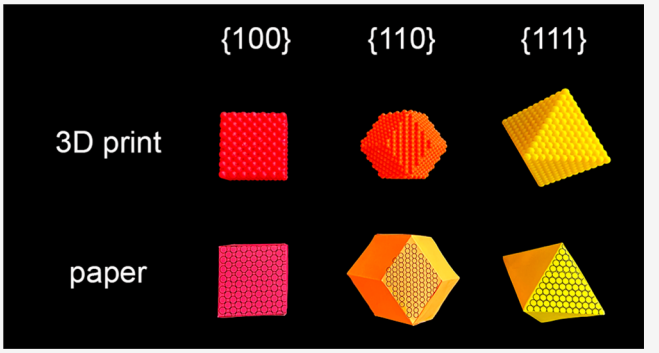

KEYWORDS: *Upper-Division Undergraduate, Graduate Education/Research, Inorganic Chemistry, Physical Chemistry, Interdisciplinary/Multidisciplinary, Hands-On Learning/Manipulatives, Solid State Chemistry*

INTRODUCTION

Nanomaterials (solid state particles with at least one dimension less than 100 nm in length) can demonstrate remarkable physical and chemical properties influenced by the size, shape, composition, and architecture (or structure) of the particles. Students at all levels have studied the striking visual effects that result when the dimensions of a metal are reduced to the nanoscale.[1−3] In the past 20 years, increasing control of solution-phase syntheses to create nanoparticles bound by different crystalline surfaces (or facets) has greatly expanded our understanding of how metal nanoparticle shape also affects chemical and physical properties. Nanoparticle shape control is a major area of chemistry research with applications in sensing, catalysis, medicine, and more.

The opportunities arising from nanoparticles with shape control become evident when considering results from fundamental surface science, which demonstrated that some reactions are more favorable on certain crystalline surfaces than on others. For example, one Pt metal surface can catalyze the hydrogenation of benzene to form cyclohexane and cyclohexene while another Pt surface produces only cyclohexene.[4] This effect was first demonstrated for single-crystalline surfaces but has since been extended to Pt nanoparticles.[5] Control over nanoparticle shape to preferentially favor one or more crystal facet(s) has allowed the study of both nanoscale and surface lattice plane effects.

Beyond catalysis, when nanoparticle shapes depart from spherical, their optical properties change dramatically. Nanoparticles of gold, silver, and copper demonstrate localized surface plasmon resonance (LSPR) in the visible range. Conduction electrons confined to the nanoparticle surface are excited into resonance by incident electromagnetic radiation. While spherical particles absorb light at a single resonant energy, anisotropic shapes such as nanorods, nanoprisms, and nanostars can feature two or more LSPR peaks as surface electrons oscillate along different axes within the material. Recent lab experiments have demonstrated how students can synthesize gold and silver nanorods, nanoprisms, and nanostars and then explore the effect of nanoparticle shape on optical properties using UV−visible spectroscopy and the observed colors of the nanoparticle aqueous solutions.[6−9] These recent experiments all make use of the seed-mediated nanoparticle growth method in which chemical additives are used to alter the crystal facet surface energies of a preformed seed crystal, thus controlling the shape of the resulting nanoparticles.

Received: April 26, 2023
Revised: July 10, 2023
Published: July 31, 2023

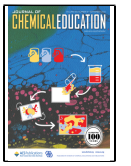

https://doi.org/10.1021/acs.jchemed.3c00371
J. Chem. Educ. 2023, 100, 3425−3433

Figure 1. A lattice of tree seedlings creates rows of seedlings that are (a) at an angle and (b) perpendicular to the edge of the field. The two photographs were taken from a single standpoint, with the photographer rotating position to view the lattice along different angles. (Photos by author AKB.) (c) A three-dimensional lattice of atoms can also be viewed along crystalline planes.

Control over nanoparticle shape has greatly expanded the number and type of studies available to the chemistry community. This Account will introduce the nomenclature system used to label crystalline planes and directions of crystal growth, provide templates for paper cut-and-fold and 3D printable nanoparticle visual aids for use in instruction, and highlight the centrality of crystal planes and facets to metal nanoparticle shape control. The importance of nanocrystal shape control to the study of catalysis, plasmonics, and sensing coupled with the visual appeal of nanocrystal polyhedral shapes will be of interest to inorganic, physical, and materials chemistry instructors and students.

■ CRYSTAL LATTICES AND THEIR PLANES

Atoms or molecules in crystalline solids form a pattern that repeats in three dimensions over an extended distance. Viewing the pattern from different angles reveals different sets of repeating parallel planes. A two-dimensional example is shown in Figure 1a,b, where a grid of tree seedlings viewed from different angles shows sets of repeating parallel rows. The concept is extended in three dimensions in crystalline solids, as shown in Figure 1c.

The planes within crystalline lattices play a critical role in materials science and solid-state chemistry. An understanding of crystal planes, facets, and directions of growth as well as the system used to name (or index) them is essential for anyone learning about or conducting research in these fields. Incident X-rays diffract from layers of atoms in a crystal, with the results depending on the spacing between the crystalline planes and the arrangement of atoms within a given plane. At incident angles for which diffraction generates constructive interference, peaks of X-ray intensity are detected. The patterns of peaks resulting from powder or single crystal X-ray diffraction studies are used to identify material phases and/or provide molecular information including bond lengths and bond angles.[10−12] Each X-ray diffraction peak is labeled with the family of planes that generates it using a three-digit address. The same nomenclature system is used to describe the surfaces (or facets) of crystalline solids, which are important to understanding control of nanoparticle shape.

Solid-state chemistry is a visually appealing subject, and visual aids can help students imagine both the structure of the unit cell and the extended crystal lattice. The unit cell is a repeat unit of a crystal that, when continually translated in the x, y, and z directions by the length of the unit cell, generates the entire crystal lattice. It is important to note that the unit cell is not necessarily the smallest repeat unit in the crystal lattice. Primitive cells are unit cells that are defined as containing only one lattice point and in many cases are smaller than the unit cell chosen to represent the crystal structure. A plethora of suggestions for visual aids to demonstrate individual unit cells and extended crystal structures (called Bravais lattices) are available, making use of a diverse toolbox of construction materials including, but not limited to, marbles or pressed cork balls held together with rubber cement,[13,14] magnet-embedded silicone balls,[15] and ping pong balls and tape.[16] Students can construct their own models of individual unit cells and extended Bravais lattices using paper cut-and-fold models or by 3D printing.[17−20] Many instructors incorporate the solid-state model kit previously available from the Institute for Chemical Education into their teaching.[21,22] Together, these models provide strong visual representations of unit cells and extended crystal lattices, but they do not explicitly highlight or provide instruction about crystalline lattice planes and how crystal facet surface energy can be used to control nanoparticle shape.

In addition to visual aids, a large number of learning activities have been developed to teach crystal structure and crystallography.[23] Some available experiments introduce crystal structure and X-ray diffraction concepts using 2D colloidal crystals formed by relatively large silica or polystyrene spheres.[24−26] These larger-scale crystals make instruction accessible by using optical microscopy and visible laser light to replace X-ray techniques. Other experiments provide students with hands-on experience using powder X-ray diffraction to characterize solid-state and/or nanomaterials that they have synthesized.[27−31] By necessity, many of these classroom or laboratory activities refer to crystal planes, but none provide explicit instruction about how they are defined.

Although an understanding of crystal planes is essential to teaching and learning solid-state chemistry, the number of available resources (i.e., visual aids or articles other than textbooks) addressing these topics is limited. Kennard briefly described the construction of wooden models to demonstrate lattice planes in 1979.[32] Since then, the advent of computers has enabled screen-based simulations including animations to visualize extended lattices,[33−35] a web-based interface for a Cartesian coordinate editor that allows students to slice solids along lattice planes,[36] and a tutorial Web site specifically focused on defining lattice planes.[37,38] This article will introduce two types of hands-on visual aids that instructors can use to emphasize the most common lattice planes found as the facets of metal nanoparticles crystallized in the face-centered cubic crystal structure. Understanding the differences between these planes is critical to understanding how

https://doi.org/10.1021/acs.jchemed.3c00371
J. Chem. Educ. 2023, 100, 3425−3433

nanoparticle growth can be controlled to yield shapes, such as cubes, rhombic dodecahedra, and octahedra.

DEFINING AND INDEXING LATTICE PLANES AND CRYSTAL FACETS

100, $3\bar{2}1$, 725, 010... To the novice solid-state chemist, the system used to index lattice planes can look like a mysterious address or a jumble of numbers. How do these numbers describe the planes of atoms or molecules in a crystal? The crystallographic notation system designating the sets of planes in a crystalline lattice uses three numbers (hkl) referred to as Miller indices. Hexagonal crystal systems require a fourth index, i, which is defined as $-(h + k)$. British mineralogist William Hallowes Miller developed the concept in 1839, building on previous work by a German mineralogist, Christian Samuel Weiss. The most mathematically rigorous approach to defining Miller indices references the reciprocal lattice and is described in detail in solid state physics textbooks.[39] An alternative method relies on examining the intersection of a representative plane with the edges of a single unit cell in the crystal.[10,12,40] The intercept approach is sufficient for most solid-state chemistry work and is described herein.

The process of indexing a set of parallel lattice planes is demonstrated in Figure 2. The examples presented here will be restricted to cubic unit cells for which the lengths of the edges a, b, and c are equal, and the angles between all unit cell edges are 90°. First, an origin point is assigned for the unit cell (typically a corner) and the x, y, and z axis directions relative to the origin are defined using the right-hand convention (Figure 2a). For a cubic system, the unit cell lengths a, b, and c lie along the x, y, and z directions, respectively (Figure 2b).

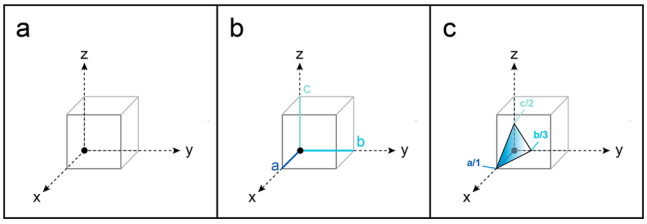

Figure 2. Generation of Miller indices from the points of intersection between a plane and the unit cell with respect to the unit cell edge lengths. The light gray outline indicates the borders of a cubic unit cell; the front face is darker to aid in visualization. (a) x, y, and z axes are defined using the right-hand convention. The origin is chosen such that the plane to be indexed does not pass through it. (b) For a cubic crystal, the unit cell's edge lengths a, b, and c (the dimensions of the unit cell) are defined along the x, y, and z axes, respectively. (c) A section of a (132) plane intersects the x axis at $a/1$, the y axis at $b/3$, and the z axis at $c/2$.

Then, a single representative plane from the set of parallel planes is selected to be indexed; choose the plane in the set that intersects the unit cell closest to the origin without passing through it. Figure 2c illustrates only a small section of one plane, highlighting the points at which the plane intersects the unit cell. This plane extends in two dimensions throughout the entire crystal and is one plane among a set of parallel planes. To index a given plane, the point at which the plane intercepts the unit cell along each axis is determined and the intersection coordinate is expressed in terms of a fraction of the length of the unit cell along that axis. For example, the plane shown in Figure 2c intersects the x axis at $a/1$, the y axis at $b/3$, and the z axis at $c/2$, with intercepts of 1, 1/3, and 1/2. The reciprocals of the intercepts with the a, b, and c unit cell lengths are Miller indices h, k, and l. Taking the reciprocals of the intersection values generates the Miller indices for the plane in Figure 2c: h = 1, k = 3, and l = 2. The plane is said to be a member of the (132) set of parallel planes. It is important to realize that not all lattice planes actually contain atoms.

Special circumstances are illustrated in Boxes 1 and 2. If a plane selected for indexing does not intercept an axis at all (i.e., it is parallel to the axis), its interception point is considered to be infinity and the h, k, or l value is $1/\infty$ = zero. If a plane intersects an axis along a negative direction relative to the origin, its h, k, or l value is negative, as indicated by a horizontal bar over the number. Miller indices are always integers, so if a plane intersects an edge at a point where the reciprocal of $1/a$ is not an integer, then all three intercepts are multiplied by a common number to achieve integer Miller indices.

The Miller indices for a set of planes are pronounced out loud by listing the h, k, and l numbers in sequence. For example, the (100) set of planes is called the "one zero zero" set. The bar above the number used to indicate a negative

Box 1. Miller Indices Equal to Zero

Consider a cubic unit cell with the origin defined at the dot in the rear left corner.

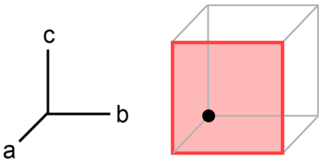

The highlighted lattice plane intersects the unit cell at $a/1$. It is parallel to both the b and c axes; therefore, it never intersects them. The intersection point for the b and c axes is considered to be infinity, and the k and l Miller indices are 0. This plane is part of the (100) set of planes.

Box 2. Negative Miller Indices

This lattice plane intersects the origin (indicated by a dot).

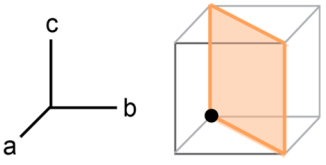

In order to index the set of planes, we shift perspective to the next plane in the set that is closest to the origin without intersecting it.

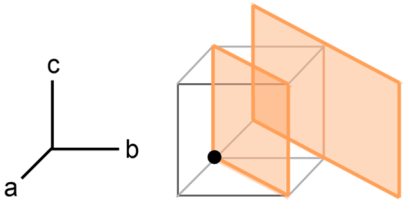

This second plane intersects the unit cell at $-a/1$, $b/1$, and is parallel to the c edge. These planes belong to the $(\bar{1}10)$ set of planes.

https://doi.org/10.1021/acs.jchemed.3c00371
J. Chem. Educ. 2023, 100, 3425−3433

Table 1. Miller Index Notation

Designation	Meaning	Example[a]
(*hkl*)	A set of parallel planes across a crystal lattice	(100) = 
{*hkl*}	A family of equivalent sets of planes	{100} = 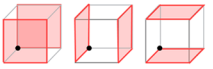
[*hkl*]	A direction of growth perpendicular to a lattice plane	[010] = 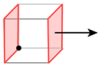
<*hkl*>	A family of equivalent directions of growth	<100> = 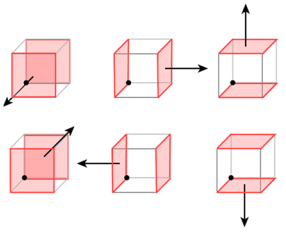

[a]All examples are given for a cubic crystal system. The origin is indicated with a dot.

Miller index is pronounced "bar", as in "one, one bar, two" for the $(1\bar{1}2)$ set of planes.

The *hkl* indices can refer to sets of parallel planes, families of equivalent sets of planes, directions of crystal growth, and families of equivalent directions of crystal growth. Table 1 summarizes the notation used to differentiate these concepts.

Parentheses are used to indicate a single set of parallel lattice planes extending in all directions throughout a crystal. The example in the first row of Table 1 shows two of the (100) planes in a cubic crystal lattice. The planes contain the front and back faces of the unit cell, but the full (100) set includes all planes in this orientation spaced equidistantly throughout the crystal lattice and extending to the edge of the crystal. Because the unit cell lengths *a*, *b*, and *c* are equal for a cubic system, the (010) and (001) sets of planes are symmetrically equivalent to the (100) set by rotation of the axis system. Together, the (100), (010), and (001) sets of planes are said to comprise the {100} family of planes (Table 1, second row). It is important to note that these sets of planes would not all be equivalent in a tetragonal lattice, for example, in which $a = b \neq c$. In a cubic system, there are six sets of planes that make up the {110} family and four sets of planes that make up the {111} family. Diagrams of each of these families of planes are included in the Supporting Information.

Miller indices can also be used to indicate directions of crystal growth. For cubic systems, these directions of growth are normal to the plane surface that shares the same set of Miller indices. For example, growth in the [010] direction proceeds in the positive *y* direction (Table 1, third row). Because growth in the positive *y* direction and growth in the negative *y* direction are unique directions, six growth directions make up the ⟨100⟩ family of growth directions, as shown in the fourth row of Table 1. The surfaces of single crystal nanoparticles are bound by lattice planes, and nanoparticle growth can be controlled by understanding the surface free energies of these lattice planes.

FACE CENTERED CUBIC NANOPARTICLES

The face-centered cubic (fcc) crystal packing structure is common among the metals Au, Ag, Pt, Rh, Ir, Pd, Ni, and Cu, which have been the focus of most nanoparticle shape control studies to date. The fcc structure is one of the most common crystal structures and arises from alternating layers of hexagonally close packed atoms; a review of the fcc structure is included in the Supporting Information.

Figure 3 demonstrates how three families of planes in the fcc extended crystal lattice are defined relative to the unit cell, how atoms are packed on the surfaces of these planes, and how these planes can form the crystal facets of three nanoparticle shapes. The low-index planes (in which all Miller indices are either 1 or 0) are the most thermodynamically stable in the fcc

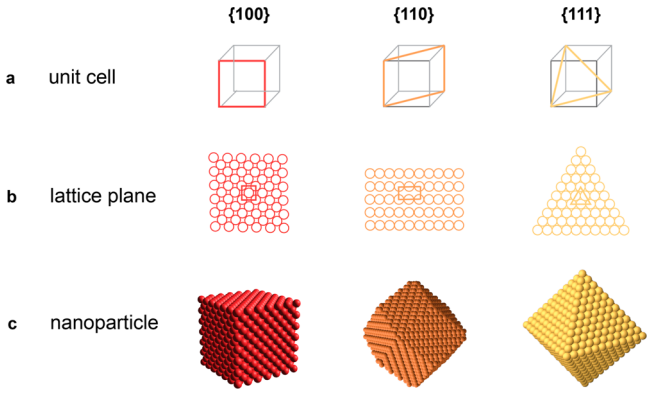

Figure 3. (a) The fcc unit cell can be sliced along the {100}, {110}, and {111} lattice planes. (b) The 2D atom density exposed by each of the three types of lattice planes; the slice of a single unit cell is outlined. (c) The nanoparticle shapes that are bound by each type of lattice plane. Note that the {110} crystal facet is rotated in forming the rhombic dodecahedron facet compared to the angle used to slice the unit cell along the {110} planes. Red, orange, and yellow colors are used to differentiate the {100}, {110}, and {111} lattice planes; all atoms are of a single metal element.

https://doi.org/10.1021/acs.jchemed.3c00371
J. Chem. Educ. 2023, 100, 3425−3433

crystal system (Figure 3a). The {100} planes align with the faces of the fcc unit cell, as it is most typically drawn. The {110} planes are each found by slicing the extended lattice along a diagonal of a unit cell face, and the {111} planes each cut the unit cell along a body diagonal.

Figure 3b shows the extended 2D arrays of atoms exposed by each of the three low-index planes; each array represents much more than a single unit cell. The 2D arrays shown in Figure 3b demonstrate that each of these planes features a different 2D density of metal atoms, with atoms occupying approximately 79% of the area of the face for the {100} planes, 56% for the {110} planes, and 91% for the {111} planes. Students can calculate and compare these densities to help convince themselves that the crystal planes would display different chemical behavior. Example calculations are included in the Supporting Information.

The surface energy of a crystalline plane is the excess free energy of atoms on the surface as compared to atoms buried in the bulk of the material.[41] To cut a bulk crystal along a lattice plane, metal−metal bonds must be broken. Planes in which atoms are more closely packed within the plane require fewer bonds to be broken between the planes in order to form. In the fcc structure, all atoms have 12 nearest neighbors in three dimensions. However, dividing a bulk fcc metal along the (111) plane requires the breaking of 3 metal−metal bonds per atom in the plane, while forming (100) and (110) planes requires the breaking of 4 and 6 bonds per atom, respectively. Generally, planes in which atoms are more densely packed have lower surface energies and are, thus, more thermodynamically stable. Collectively, the three low-index sets of planes have the lowest surface energies of all planes in the fcc crystal structure. For nanoparticles, the surface area of each facet also contributes to the total surface energy of the particle.

A plane that contributes to the outer surface of a nanoparticle is called a facet. Nanoparticles of different shapes have different crystal facets exposed to the outer world, and nanoparticles of fcc metals form the shapes shown in Figure 3c when bound by the low-index fcc lattice planes. Cubes are bound by six facets of the {100} family, rhombic dodecahedra by 12 {110} facets, and octahedra by eight {111} facets. The three low-index facets have surface free energies in the order {111} < {100} < {110}, and these relative energies can be deployed to inhibit crystal growth in some direction(s) and encourage growth in other direction(s), thus controlling the shape of a growing nanoparticle.[42] The Supporting Information includes files for 3D printed models demonstrating the cubes, rhombic dodecahedra, and octahedra nanoparticle shapes that are bound by each of these types of planes. The images in Figure 3c and the 3D printed models depict idealized structures; the corners and edges of actual nanoparticles would have rounded edges and corners.

SHAPE CONTROL OF NANOPARTICLE GROWTH

Metal nanoparticles form from metal salt solutions through the processes of nucleation and growth. In nucleation, metal ions are reduced and aggregate in solution (homogeneous nucleation) or deposit on a pre-existing surface (heterogeneous nucleation). Chemists have found that nanocrystal shape can be much better controlled if the particles are grown in a two-step seed-mediated synthesis, and a number of excellent reviews provide full details.[43−47] This two-stage approach separates nucleation and growth processes and leads to monodisperse particles (i.e., particles of uniform size) and control over shape.

First, a strong reducing agent is used to rapidly nucleate very small seeds (∼1−5 nm diameter) from an aqueous solution of a precursor salt. These seeds can have different crystalline properties and surface facets, both of which affect the ultimate shape of the particle. The description herein will focus on single-crystalline seeds in which the entire seed particle is one single crystal as opposed to seed crystals composed of multiple smaller crystals fused into one particle or crystals with structural defects. The fcc metals often form seed crystals in a truncated octahedron shape composed of both {111} and {100} facets. As the {111} family of facets has a lower surface energy, one could anticipate that it would predominate in the seed crystal shape. However, tetrahedra and octahedra bound exclusively by {111} facets have relatively large surface areas; the truncated octahedron shape leads to the minimum total surface energy for the seed crystal.[48] The degree of truncation for single crystal seeds depends on the particle size.

Scheme 1 illustrates how the different surface energies of a single-crystalline truncated octahedral seed can be used to control subsequent nanoparticle growth in the second stage of the two-step seed-mediated synthesis. In this example a quasi-spherical seed displaying all three low-index facets is used for purposes of introducing the formation of the three shapes bound by the {100}, {110}, and {111} crystal facets. After the seeds are formed, a weak reducing agent is used to slowly deposit metal atoms on the seed surface; reduction potentials are typically lower to reduce a metal onto an existing surface than to homogeneously nucleate new metal particles in solution. Growth proceeds most rapidly in the direction of the highest energy facet(s), leaving the lowest energy facet(s) as the predominant facet(s) in the resulting nanoparticle. For the seed crystal shown without any additives (top), the {110} facets (shown in orange) and {100} facets (red) are higher energy than the {111} facets (yellow). Growth proceeds in the ⟨110⟩ and ⟨100⟩ directions perpendicular to the red and

Scheme 1. Shape Control of Nanoparticle Growth from a Preformed Monometallic Seed Crystal (at Left) Featuring {100} (Red), {110} (Orange), and {111} (Yellow) Facets[a]

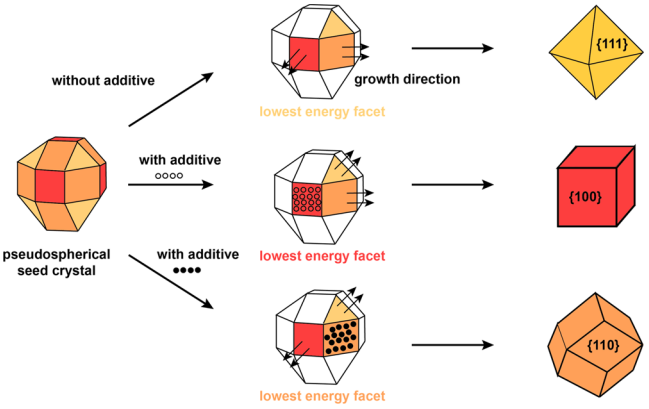

[a]In the absence of any additives, growth proceeds in the higher energy ⟨100⟩ and ⟨110⟩ directions and the resulting octahedral nanoparticle features the lowest energy {111} facets. Additives can inhibit growth in a particular direction by lowering the energy of the facet to which they adsorb, resulting in cubes with {100} facets or rhombic dodecahedra with {110} facets.

https://doi.org/10.1021/acs.jchemed.3c00371
J. Chem. Educ. 2023, 100, 3425−3433

orange facets, thereby eliminating the {110} and {100} facets and resulting in an octahedron with only {111} facets.

Chemical additives can selectively adsorb onto the {100} facets (middle) or {110} facets (bottom), passivating these facets and lowering their surface energy. This selective adsorption is dictated by the arrangement of atoms on a given facet and how the chemical additive interacts with that facet (i.e., interaction strength and orientation). Nanoparticle growth again proceeds in the higher energy directions, but now the order of the energies is different. The final result is a cube with {100} facets or a rhombic dodecahedron with {110} facets. A range of additives can be used including surfactant molecules like cetyltrimethylammonium bromide (CTAB) commonly used with Au nanoparticles, metal ions such as bromide (Br^-) commonly used with Pd nanoparticles, or polymers such as polyvinylpyrrolidone (PVP) commonly used with Ag nanoparticles. The final nanoparticle shape can be controlled by changing both the identity and the quantity of the passivating agent added. Nanoparticle growth is halted when no available metal ions remain in the growth solution, the reducing agent has been depleted, or the particles reach a size at which they are stabilized by available capping agents.

By a judicious choice of additive, the shape of the resulting nanocrystal can be controlled. Hand-held models of a cube, rhombic dodecahedron, and octahedron can be constructed by cutting and folding templates printed on cardstock or paper and then using glue or tape to hold the shape together. Undergraduate students can work in teams to complete a full set of the three models; the cube and octahedron each require about 5 min to assemble, while the more complex rhombic dodecahedron typically takes 15 min. The templates included in the Supporting Information include the option to print the atom arrangement on one face of each shape to demonstrate the crystallographic planes that form the surface of each type of nanocrystal.

APPLICATIONS OF NANOPARTICLE SHAPE CONTROL

Studies of metal nanoparticle plasmonic properties across a range of particle shapes and sizes have led to promising applications in sensing[49,50] and biological imaging and biomedicine.[51] However, the impacts of the nanoparticle shape and size can be difficult to deconvolute. For example, work correlating optical spectra to individual gold nanoparticles of five different shapes demonstrated that the LSPR behavior of each shape was more strongly related to the distance along which the plasmon resonance occurred than the nanoparticle shape.[52]

Crystal facets differ in their atom density, coordination number of surface atoms, and electronic structure, all of which impact the chemistry observed at the crystal surface. Control of nanoparticle synthesis to create materials bounded by different crystal facets has greatly expanded the knowledge of facet-based properties established by early studies, with applications in catalysis leading the way.[53]

For example, early studies of the hydrogenation of benzene on single crystalline Pt surfaces demonstrated that the Pt(100) surface produces only cyclohexane while the Pt(111) surface produces both cyclohexane and cyclohexene.[4] Sum frequency generation (SFG) surface vibrational spectroscopy was used to elucidate the mechanism of the hydrogenation reaction on platinum. For heterogeneous catalysts, the interaction of the metal surface with the intermediate species involved in the rate-determining step holds the key to controlling the reaction activity and selectivity. In forming cyclohexane from cyclohexene (the partially hydrogenated benzene) at temperatures above 370 K, the π-allyl c-C_6H_9 intermediate forms on the Pt(100) surface but does not form on the Pt(111) surface. Thus, Pt(100) converts all available cyclohexene to cyclohexane, making exclusively cyclohexane as a product while Pt(111) generates both cyclohexane (via another pathway) and cyclohexene.[4] Pt nanoparticles grown to form Pt cubes (with only {100} facets) and cuboctahedral nanoparticles (with both {100} and {111} facets) demonstrated the same selectivity as the single crystal surfaces in addition to the increase in activity expected from increasing the catalyst surface area.[5]

One future direction of nanoparticle research extends characterization from considering a group of particles *en masse* to focusing on one particle at a time. Recent work examines the reduction of CO_2 to form CO at the surfaces of three gold nanoparticle shapes.[54] Scanning electrochemical cell microscopy demonstrated that gold rhombic dodecahedra with {110} facets were more active and more selective for CO formation than gold octahedra with {111} facets and truncated ditetragonal prisms with {310}-facets. The rate-limiting step in the reduction of CO_2 is the initial transfer of an electron and a proton to CO_2 on the Au surface, forming a carboxylic acid radical bound to the Au surface (*COOH). The binding affinity of *COOH increases with lower coordination numbers of atoms on the metal surface, and Au atoms on the rhombic dodecahedron's {110} facets have a coordination number of 7, compared to 8 and 9 for atoms on the {100} and {111} facets, respectively. Thus, the CO_2 reduction reaction proceeds to a greater extent on the {110} crystal facets. The turnover frequencies of CO measured at individual Au nanoparticles confirmed the enhanced activity at the {110} facets. Furthermore, measurements demonstrated that catalytic activity can vary even between individual nanoparticles of the same shape, a phenomenon that is obscured when measurements are made in aggregate across large numbers of nanoparticles. The ability to study single nanoparticles could enable the study of other factors affecting catalytic behavior, such as subtle variations from one nanoparticle to the next (e.g., surface defects) and in the electrode surface as well as local pH and diffusion rates of reactants and products to/from the nanoparticle surface. We expect that advanced characterization techniques will expand the quantitative evaluation of facet-dependent nanoparticle properties in the future.

IMPLICATIONS FOR TEACHING

Solid-state chemistry topics are inherently interdisciplinary, and as such, they run the risk of falling through the cracks of the chemistry curriculum. The American Chemical Society (ACS) Committee on Professional Training's guidelines for chemistry departments now require that students learn about at least two types of macromolecular, supramolecular, and nanoscale systems, and departments may choose to satisfy this requirement by either distributing the content across existing courses or developing new standalone courses. The shared responsibility for instruction could lead to more opportunities to teach nanoscience topics in the chemistry curriculum.

The detailed concept maps recently developed by the ACS Exams Institute indicate that the responsibility for solid-state instruction lies primarily in the inorganic course(s), where crystal lattices, unit cells, crystal structures, and the properties

https://doi.org/10.1021/acs.jchemed.3c00371
J. Chem. Educ. 2023, 100, 3425−3433

of solids are introduced.[55] Indeed, a survey of faculty teaching inorganic chemistry found that 75% include solids and solid-state chemistry topics in their foundation-level inorganic chemistry courses.[56] Moreover, survey participants reported that coverage of materials chemistry and nanoscience topics was consistently increasing within their in-depth inorganic courses.[57] The same Exams Institute project assigned the application of solid-state knowledge to understand X-ray diffraction and index planes using Miller indices to the physical chemistry course(s).[58] Inorganic and physical chemistry textbooks reflect this division of labor; Miller indices are defined in physical chemistry texts[59−61] and mostly left out of inorganic textbooks.[62−65] Solid-state chemistry and physics textbooks provide the most comprehensive treatment of lattice planes and crystal facets.[12,39,40]

As demonstrated by the broad range of experiments and activities already published, nanomaterials topics can be blended within the inorganic or physical chemistry lecture and laboratory courses without expanding the curriculum. Alternatively, or in addition, standalone nanomaterials courses can be developed as elective courses. Some programs have offered these courses either for half credit or during an intersession.[66,67]

When appropriately presented, nanomaterials as a subject area can be of interest to students from a range of backgrounds, including college students with limited experience in chemistry.[23,68] One text provides resources for leveraging materials chemistry to teach general chemistry topics.[10] Nanomaterials chemistry courses have been developed for nonscience majors or science majors with minimal chemistry experience, and high school teachers have been trained in nanomaterials topics.[6,66,67,69−71]

In any course, nanoparticle shape control and its impact on nanoscale properties can serve as an excellent first module, using the visual appeal of crystal facets to engage student interest. Students can calculate the 2D density of atoms in the families of low-index planes in the fcc system in order to compare and contrast them.[67] Consultation with the research literature is especially appropriate as research in nanomaterials chemistry is advancing rapidly. With scaffolding and guidance from their instructor, students can learn to analyze articles from the scientific literature.[72,73] In one available literature-based activity, students evaluate different planes of Cu_2O crystals in terms of the densities of copper and oxygen atoms.[74]

This article describes the seed-mediated growth of metal nanoparticles, focusing on three shapes formed when the nanoparticles are bound by low-index facets in the face centered cubic crystal geometry. The activities described herein could be extended in a number of directions. Nanoparticles can form in other crystal systems such as body centered cubic, hexagonal close packed, or crystals with two or more types of atoms or ions. Hollow and chiral nanoparticles also present interesting optical properties.[75,76] Nanoparticles with high-index facets, in which at least one of the Miller indices is greater than 1, are generally more chemically interesting due to the high numbers of surface defects including kinks, steps, and atom vacancies. A plethora of metal nanocrystal shapes has been reported beyond those highlighted here; examples include {221}-faceted Au trisoctahedra,[77] {110}-faceted Pd concave tetrahedra,[78] and {720}-faceted Au concave cubes.[79] Many of these shapes result from seed crystals that are more complex than the single-crystalline seed model presented here. Beyond the seed-mediated approach, the nanoparticle shape can also be controlled by adjusting the surface diffusion rate of atoms deposited on certain facets and using oxidative etching and regrowth techniques.

CONCLUSION

Seed-mediated nanoparticle growth using additives to alter facet surface energies provides an excellent example of the importance of lattice planes to materials chemistry. The topics introduced here provide a foundation of knowledge to enable instructors to develop teaching materials for instruction at a number of levels and across the chemistry curriculum. Hand-held visual aids demonstrate how different crystal facets lead to different nanoparticle shapes.

ASSOCIATED CONTENT

Supporting Information

The Supporting Information is available at https://pubs.acs.org/doi/10.1021/acs.jchemed.3c00371.

Diagrams of the {100}, {110}, and {111} families of planes for a cubic crystal, introduction to fcc crystal structure, and calculation of the 2D density of atoms on the three low-index fcc lattice planes; instructions and templates for paper cut-and-fold models of cube, rhombic dodecahedron, and octahedron (PDF)

Compressed folder containing .STL files for 3D printing models of fcc cube, octahedron, and rhombic dodecahedron nanoparticles (ZIP)

AUTHOR INFORMATION

Corresponding Author

Sara E. Skrabalak − *Department of Chemistry, Indiana University, Bloomington, Indiana 47405, United States;* orcid.org/0000-0002-1873-100X; Email: sskrabal@indiana.edu

Author

Anne K. Bentley − *Department of Chemistry, Lewis & Clark College, Portland, Oregon 97219, United States;* orcid.org/0000-0003-1353-6042

Complete contact information is available at: https://pubs.acs.org/10.1021/acs.jchemed.3c00371

Notes

The authors declare no competing financial interest.

ACKNOWLEDGMENTS

The authors would like to thank Jack Googasian, Bradley Jolly (Indiana University Information Technology Group), and Justin Counts (Lewis & Clark College Information Technology) for assistance with modeling software and 3D printing. This work was supported by the US National Science Foundation (NSF CHE 2203349), Indiana University, and Lewis & Clark College.

REFERENCES

(1) Jenkins, J. A.; Wax, T. J.; Zhao, J. Seed-Mediated Synthesis of Gold Nanoparticles of Controlled Sizes To Demonstrate the Impact of Size on Optical Properties. *J. Chem. Educ.* **2017**, *94* (8), 1090−1093.

(2) Xia, Y.; Campbell, D. J. Plasmons: Why Should We Care? *J. Chem. Educ.* **2007**, *84* (1), 91.
(3) Frank, A. J.; Cathcart, N.; Maly, K. E.; Kitaev, V. Synthesis of Silver Nanoprisms with Variable Size and Investigation of Their Optical Properties: A First-Year Undergraduate Experiment Exploring Plasmonic Nanoparticles. *J. Chem. Educ.* **2010**, *87* (10), 1098−1101.
(4) Bratlie, K. M.; Kliewer, C. J.; Somorjai, G. A. Structure Effects of Benzene Hydrogenation Studied with Sum Frequency Generation Vibrational Spectroscopy and Kinetics on Pt(111) and Pt(100) Single-Crystal Surfaces. *J. Phys. Chem. B* **2006**, *110* (36), 17925−17930.
(5) Bratlie, K. M.; Lee, H.; Komvopoulos, K.; Yang, P.; Somorjai, G. A. Platinum Nanoparticle Shape Effects on Benzene Hydrogenation Selectivity. *Nano Lett.* **2007**, *7* (10), 3097−3101.
(6) Vinnacombe-Willson, G. A.; Chiang, N.; Weiss, P. S.; Tolbert, S. H.; Scarabelli, L. Seeded-Growth Experiment Demonstrating Size- and Shape-Dependence on Gold Nanoparticle−Light Interactions. *J. Chem. Educ.* **2021**, *98* (2), 546−552.
(7) Panzarasa, G. Just What Is It That Makes Silver Nanoprisms so Different, so Appealing? *J. Chem. Educ.* **2015**, *92* (11), 1918−1923.
(8) Ferraro, G.; Fratini, E. A Simple Synthetic Approach To Prepare Silver Elongated Nanostructures: From Nanorods to Nanowires. *J. Chem. Educ.* **2019**, *96* (3), 553−557.
(9) Pérez-Mariño, Á. M.; Blanco, M. C.; Buceta, D.; López-Quintela, M. A. Using Silver Nanoclusters as a New Tool in Nanotechnology: Synthesis and Photocorrosion of Different Shapes of Gold Nanoparticles. *J. Chem. Educ.* **2019**, *96* (3), 558−564.
(10) *Teaching General Chemistry: A Materials Science Companion*; Ellis, A. B., Ed.; American Chemical Society: Washington, DC, 1993.
(11) Cullity, B. D.; Stock, S. R. *Elements of X-Ray Diffraction*, 3rd ed.; Prentice Hall: Upper Saddle River, NJ, 2001.
(12) West, A. R. *Basic Solid State Chemistry*, 2nd ed.; John Wiley & Sons: New York, 1999.
(13) Scattergood, A. The Making of Crystal Lattice and Unit Cell Models. *J. Chem. Educ.* **1937**, *14* (3), 140.
(14) Hauser, E. A. A Simple Method of Building Close-Packed Molecular and Crystal Models. *J. Chem. Educ.* **1941**, *18* (4), 164.
(15) Ma, Y.-Z.; Yang, Z.-L.; Wang, Y.; Wang, H.-H.; Tian, S. J. Using Magnet-Embedded Silicone Balls to Construct Stable Models for Close-Packed Crystal Structures. *J. Chem. Educ.* **2020**, *97* (11), 4063−4068.
(16) Elsworth, C.; Li, B. T. Y.; Ten, A. Constructing Cost-Effective Crystal Structures with Table Tennis Balls and Tape That Allows Students To Assemble and Model Multiple Unit Cells. *J. Chem. Educ.* **2017**, *94* (7), 827−828.
(17) Libonati, F.; Graziosi, S.; Ballo, F.; Mognato, M.; Sala, G. 3D-Printed Architected Materials Inspired by Cubic Bravais Lattices. *ACS Biomater. Sci. Eng.* **2023**, *9*, 3935.
(18) Birk, J. P.; Yezierski, E. J.; Laing, M. Paper-and-Glue Unit Cell Models. *J. Chem. Educ.* **2003**, *80* (2), 157.
(19) Sein, L. T., Jr.; Sein, S. E. Lattice Entertain You: Paper Modeling of the 14 Bravais Lattices on YouTube. *J. Chem. Educ.* **2015**, *92* (8), 1419−1421.
(20) Rodenbough, P. P.; Vanti, W. B.; Chan, S.-W. 3D-Printing Crystallographic Unit Cells for Learning Materials Science and Engineering. *J. Chem. Educ.* **2015**, *92* (11), 1960−1962.
(21) Crowder, N. Solid State Models with ICE Solid State Model Kits. https://www.ionicviper.org/classactivity/solid-state-models-ice-solid-state-model-kits (accessed on February 1, 2023).
(22) Sunderland, D. P. Studying Crystal Structures through the Use of Solid-State Model Kits. *J. Chem. Educ.* **2014**, *91* (3), 432−436.
(23) Caro, V.; Carter, B. A.; Millunchick, J.; Reeves, S. Teaching Crystal Structures in Undergraduate Courses: A Systematic Review from a Disciplinary Literacy Perspective. *Chem. Educ. Res. Pract.* **2023**, *24*, 394.
(24) Bosse, S. A.; Loening, N. M. Using Two-Dimensional Colloidal Crystals To Understand Crystallography. *J. Chem. Educ.* **2008**, *85* (1), 93.
(25) Abrams, N. M.; Schaak, R. E. Self-Assembled Colloidal Crystals: Visualizing Atomic Crystal Chemistry Using Microscopic Analogues of Inorganic Solids. *J. Chem. Educ.* **2005**, *82* (3), 450.
(26) Xia, Y.; Campbell, D. J.; Lisensky, G. C. Powder Diffraction Simulated by a Polycrystalline Film of Spherical Colloids. *J. Chem. Educ.* **2006**, *83* (11), 1638.
(27) Lisensky, G. C.; Dauzvardis, F.; Young, M. M. K. Periodic Properties Illustrated by CH3NH3Pb(I1−XBrx)3 Solid Solution Perovskite Semiconductors. *J. Chem. Educ.* **2021**, *98* (7), 2392−2397.
(28) Butera, R. A.; Waldeck, D. H. X-Ray Diffraction Investigation of Alloys. *J. Chem. Educ.* **1997**, *74* (1), 115.
(29) Varberg, T. D.; Skakuj, K. X-Ray Diffraction of Intermetallic Compounds: A Physical Chemistry Laboratory Experiment. *J. Chem. Educ.* **2015**, *92* (6), 1095−1097.
(30) Koenig, E.; Jacobs, A.; Lisensky, G. Properties of Semiconductors: Synthesis of Oriented ZnO for Photoelectrochemistry and Photoremediation. *J. Chem. Educ.* **2017**, *94* (6), 738−742.
(31) Martín-Ramos, P.; Susano, M.; Gil, F. P. S. C.; Pereira da Silva, P. S.; Martín-Gil, J.; Silva, M. R. Facile Synthesis of Three Kobolds: Introducing Students to the Structure of Pigments and Their Characterization. *J. Chem. Educ.* **2018**, *95* (8), 1340−1344.
(32) Kennard, C. H. L.; Bretherton, L. Teaching Aids Illustrating the Concept of Miller Index. *J. Chem. Educ.* **1979**, *56* (1), 38.
(33) Johnston, D. Crystallographic Resources at Otterbein University. https://crystals.symotter.org/ (accessed on June 24, 2023).
(34) Lisensky, G. Solid State Stoichiometry Online. https://www.ionicviper.org/web-resources-and-apps/solid-state-stoichiometry-online (accessed on February 1, 2023).
(35) Lisensky, G. Solid State Stoichiometry Online. https://www.ionicviper.org/class-activity/close-packing-activity (accessed on February 1, 2023).
(36) Polik, W. F.; Schmidt, J. R. WebMO: Web-Based Computational Chemistry Calculations in Education and Research. *WIREs Computational Molecular Science* **2022**, *12* (1), No. e1554.
(37) McCaffrey, V. Introduction to Miller Indices. https://www.ionicviper.org/web-resources-and-apps/introduction-miller-indices (accessed on February 1, 2023).
(38) Lattice Planes and Miller Indices. https://www.doitpoms.ac.uk/tlplib/miller_indices/index.php (accessed on February 1, 2023).
(39) Ashcroft, N. W.; Mermin, N. D. *Solid State Physics*; Holt, Rinehart and Winston: New York, 1976.
(40) Tilley, R. J. D. *Crystals and Crystal Structures*; John Wiley: Hoboken, NJ, 2006.
(41) *Introduction to Nanoscience*; Hornyak, G. L., Ed.; CRC Press: Boca Raton, 2008.
(42) Wang, Z. L. Transmission Electron Microscopy of Shape-Controlled Nanocrystals and Their Assemblies. *J. Phys. Chem. B* **2000**, *104* (6), 1153−1175.
(43) Skrabalak, S. E. Symmetry in Seeded Metal Nanocrystal Growth. *Acc. Mater. Res.* **2021**, *2* (8), 621−629.
(44) Xia, Y.; Gilroy, K. D.; Peng, H.-C.; Xia, X. Seed-Mediated Growth of Colloidal Metal Nanocrystals. *Angew. Chem., Int. Ed.* **2017**, *56* (1), 60−95.
(45) Tao, A. R.; Habas, S.; Yang, P. Shape Control of Colloidal Metal Nanocrystals. *Small* **2008**, *4* (3), 310−325.
(46) Xia, Y.; Xiong, Y.; Lim, B.; Skrabalak, S. E. Shape-Controlled Synthesis of Metal Nanocrystals: Simple Chemistry Meets Complex Physics? *Angew. Chem., Int. Ed.* **2009**, *48* (1), 60−103.
(47) Personick, M. L.; Mirkin, C. A. Making Sense of the Mayhem behind Shape Control in the Synthesis of Gold Nanoparticles. *J. Am. Chem. Soc.* **2013**, *135* (49), 18238−18247.
(48) Wulff, G. *XXV. Zur Frage Der Geschwindigkeit Des Wachsthums Und Der Auflösung Der Krystallflächen* **1901**, *34* (1−6), 449−530.
(49) Anker, J. N.; Hall, W. P.; Lyandres, O.; Shah, N. C.; Zhao, J.; Van Duyne, R. P. Biosensing with Plasmonic Nanosensors. *Nat. Mater.* **2008**, *7* (6), 442−453.
(50) Lee, K.-S.; El-Sayed, M. A. Gold and Silver Nanoparticles in Sensing and Imaging: Sensitivity of Plasmon Response to Size, Shape,

https://doi.org/10.1021/acs.jchemed.3c00371
J. Chem. Educ. 2023, 100, 3425−3433

and Metal Composition. *J. Phys. Chem. B* **2006**, *110* (39), 19220−19225.
(51) Jain, P. K.; Huang, X.; El-Sayed, I. H.; El-Sayed, M. A. Noble Metals on the Nanoscale: Optical and Photothermal Properties and Some Applications in Imaging, Sensing, Biology, and Medicine. *Acc. Chem. Res.* **2008**, *41* (12), 1578−1586.
(52) Ringe, E.; Langille, M. R.; Sohn, K.; Zhang, J.; Huang, J.; Mirkin, C. A.; Van Duyne, R. P.; Marks, L. D. Plasmon Length: A Universal Parameter to Describe Size Effects in Gold Nanoparticles. *J. Phys. Chem. Lett.* **2012**, *3* (11), 1479−1483.
(53) Shi, Y.; Lyu, Z.; Zhao, M.; Chen, R.; Nguyen, Q. N.; Xia, Y. Noble-Metal Nanocrystals with Controlled Shapes for Catalytic and Electrocatalytic Applications. *Chem. Rev.* **2021**, *121* (2), 649−735.
(54) Jeong, S.; Choi, M.-H.; Jagdale, G. S.; Zhong, Y.; Siepser, N. P.; Wang, Y.; Zhan, X.; Baker, L. A.; Ye, X. Unraveling the Structural Sensitivity of CO2 Electroreduction at Facet-Defined Nanocrystals via Correlative Single-Entity and Macroelectrode Measurements. *J. Am. Chem. Soc.* **2022**, *144* (28), 12673−12680.
(55) Marek, K. A.; Raker, J. R.; Holme, T. A.; Murphy, K. L. The ACS Exams Institute Undergraduate Chemistry Anchoring Concepts Content Map III: Inorganic Chemistry. *J. Chem. Educ.* **2018**, *95* (2), 233−237.
(56) Raker, J. R.; Reisner, B. A.; Smith, S. R.; Stewart, J. L.; Crane, J. L.; Pesterfield, L.; Sobel, S. G. Foundation Coursework in Undergraduate Inorganic Chemistry: Results from a National Survey of Inorganic Chemistry Faculty. *J. Chem. Educ.* **2015**, *92* (6), 973−979.
(57) Raker, J. R.; Reisner, B. A.; Smith, S. R.; Stewart, J. L.; Crane, J. L.; Pesterfield, L.; Sobel, S. G. In-Depth Coursework in Undergraduate Inorganic Chemistry: Results from a National Survey of Inorganic Chemistry Faculty. *J. Chem. Educ.* **2015**, *92* (6), 980−985.
(58) Holme, T. A.; Reed, J. J.; Raker, J. R.; Murphy, K. L. The ACS Exams Institute Undergraduate Chemistry Anchoring Concepts Content Map IV: Physical Chemistry. *J. Chem. Educ.* **2018**, *95* (2), 238−241.
(59) *Physical Chemistry: Principles and Applications in Biological Sciences*, 5th ed.; Tinoco, I., Tinoco, I., Eds.; Pearson: Boston, 2014.
(60) Atkins, P. W.; de Paula, J.; Keeler, J. *Atkins' Physical Chemistry*, 11th ed.; Oxford University Press: Oxford, United Kingdom; New York, NY, 2018.
(61) Levine, I. N. *Physical Chemistry*, 6th ed.; McGraw-Hill: Boston, 2009.
(62) Rayner-Canham, G.; Overton, T. *Descriptive Inorganic Chemistry*, 6th ed.; W.H. Freeman and Company, a Macmillan Higher Education Company: New York, 2014.
(63) Miessler, G. L.; Fischer, P. J.; Tarr, D. A. *Inorganic Chemistry*, 5th ed.; Pearson: Boston, 2014.
(64) *Shriver & Atkins' Inorganic Chemistry*, 5th ed.; Atkins, P. W., Ed.; Oxford University Press: Oxford; New York, 2010.
(65) Housecroft, C. E. *Inorganic Chemistry*, 5th ed.; Pearson: Harlow, England; New York, 2018.
(66) Walters, K. A.; Bullen, H. A. Development of a Nanomaterials One-Week Intersession Course. *J. Chem. Educ.* **2008**, *85* (10), 1406.
(67) Bentley, A. K.; Imatani, G. Nanomaterials Chemistry: A Half-Credit Course for Science Majors. *J. Nano. Ed.* **2013**, *4*, 33−40.
(68) Greenberg, A. Integrating Nanoscience into the Classroom: Perspectives on Nanoscience Education Projects. *ACS Nano* **2009**, *3* (4), 762−769.
(69) Park, E. J. Nanotechnology Course Designed for Non-Science Majors To Promote Critical Thinking and Integrative Learning Skills. *J. Chem. Educ.* **2019**, *96* (6), 1278−1282.
(70) Porter, L. A., Jr. Chemical Nanotechnology: A Liberal Arts Approach to a Basic Course in Emerging Interdisciplinary Science and Technology. *J. Chem. Educ.* **2007**, *84* (2), 259.
(71) Blonder, R. The Story of Nanomaterials in Modern Technology: An Advanced Course for Chemistry Teachers. *J. Chem. Educ.* **2011**, *88* (1), 49−52.
(72) Maxwell, D. N.; Spencer, J. L.; Teich, E. A.; Cooke, M.; Fromwiller, B.; Peterson, N.; Nicholas-Figueroa, L.; Shultz, G. V.; Pratt, K. A. A Guided-Inquiry Activity for Introducing Students to Figures from Primary Scientific Literature. *J. Chem. Educ.* **2023**, *100*, 1788.
(73) Reisner, B. A.; Stewart, J. L. The Literature Discussion: A Signature Pedagogy for Chemistry. In *Advances in Teaching Inorganic Chemistry Vol. 1: Classroom Innovations and Faculty Development*; ACS Symposium Series; American Chemical Society: Washington, DC, 2020; Vol. *1370*, pp 3−20. DOI: 10.1021/bk-2020-1370.ch002.
(74) Steinmiller, E. Copper Oxide Crystal Growth. https://www.ionicviper.org/literature-discussion/copper-oxide-crystal-growth (accessed on February 1, 2023).
(75) Lee, H.-E.; Ahn, H.-Y.; Mun, J.; Lee, Y. Y.; Kim, M.; Cho, N. H.; Chang, K.; Kim, W. S.; Rho, J.; Nam, K. T. Amino-Acid- and Peptide-Directed Synthesis of Chiral Plasmonic Gold Nanoparticles. *Nature* **2018**, *556* (7701), 360−365.
(76) Jenkins, S. V.; Gohman, T. D.; Miller, E. K.; Chen, J. Synthesis of Hollow Gold−Silver Alloyed Nanoparticles: A "Galvanic Replacement" Experiment for Chemistry and Engineering Students. *J. Chem. Educ.* **2015**, *92* (6), 1056−1060.
(77) Ma, Y.; Kuang, Q.; Jiang, Z.; Xie, Z.; Huang, R.; Zheng, L. Synthesis of Trisoctahedral Gold Nanocrystals with Exposed High-Index Facets by a Facile Chemical Method. *Angew. Chem., Int. Ed.* **2008**, *47* (46), 8901−8904.
(78) Huang, X.; Tang, S.; Zhang, H.; Zhou, Z.; Zheng, N. Controlled Formation of Concave Tetrahedral/Trigonal Bipyramidal Palladium Nanocrystals. *J. Am. Chem. Soc.* **2009**, *131* (39), 13916−13917.
(79) Zhang, J.; Langille, M. R.; Personick, M. L.; Zhang, K.; Li, S.; Mirkin, C. A. Concave Cubic Gold Nanocrystals with High-Index Facets. *J. Am. Chem. Soc.* **2010**, *132* (40), 14012−14014.

https://doi.org/10.1021/acs.jchemed.3c00371
J. Chem. Educ. 2023, 100, 3425−3433